J Mater Sci (2006) 41:7492–7497
DOI 10.1007/s10853-006-0803-3

In-situ thermal polymerization of rechargeable lithium batteries with poly(methyl methacrylate) based gel-polymer electrolyte

Y. F. Zhou · S. Xie · C. H. Chen

Received: 10 July 2005 / Accepted: 1 December 2005 / Published online: 19 October 2006

Abstract By heating the admixture of a commercial liquid electrolyte (LB302, 1 M solution of $LiPF_6$ in 1:1 EC/DEC), methyl methacrylate (MMA) and benzoyl peroxide (BPO, initiator), a poly(methyl methacrylate) (PMMA) based gel-polymer electrolyte (GPE) was obtained. AC impedance spectroscopy and cyclic voltammetry were used to evaluate its ionic conductivity and electrochemical stability window. Rechargeable cells $LiNi_{0.8}Co_{0.2}O_2$/Li and $LiNi_{0.8}Co_{0.2}O_2$/graphite with this MMA based GPE were also fabricated via the in-situ thermal polymerization process. This GPE exhibits a high ionic conductivity (over 10^{-3} S cm^{-1}) at room temperature. It is stable in the voltage range between 0 and 4.2 V (vs. Li^+/Li). A phenomenon of large initial cell impedance (LICI) was observed for the $LiNi_{0.8}Co_{0.2}O_2$/Li cells but not in $LiNi_{0.8}Co_{0.2}O_2$/graphite cells. After the first several cycles, the cell impedance decreases substantially and reversible charge–discharge capacity can be obtained. This in-situ polymerization method provides a way to produce GPE cells.

Introduction

In recent years, there has been an increasing need for high energy density rechargeable batteries for portable electronic equipments and other applications [1]. Lithium polymer batteries are among the most attractive choices and currently widely studied and developed. Because they can be produced in a variety of forms, a certain battery product with a required shape can be produced readily, enabling a flexible customization of portable power driven electronic equipment [2–4]. Lithium polymer batteries are fabricated with a polymer electrolyte, which can be classified into two categories, i.e. solid polymer electrolyte (SPE) and gel-polymer electrolyte (GPE) [5]. Basically, lithium batteries with SPEs can completely get rid of the problem of possible electrolyte leakage. However, SPEs exhibit lithium ion conductivities ranging from 10^{-8} to 10^{-5} S cm^{-1} at room temperature, which is not sufficient for practical applications at ambient temperature. On the other hand, lithium batteries with liquid electrolyte (conductivity above 10^{-3} S cm^{-1} at 25 °C) can operate at room temperature but have possible electrolyte leakage problem. Since lithium batteries with GPEs combine the best features of both types of batteries but have no disadvantages of lithium batteries with SPEs or liquid electrolytes, they are new-type lithium batteries with great potential of dominating market of rechargeable batteries [3–7].

PMMA based GPEs have been found to exhibit high conductivities and good mechanical strength [7–13]. In most of these researches, GPEs are prepared by first dissolving PMMA in liquid electrolyte at a temperature above 60 °C, then forming the electrolyte composite films by gel casting or immersing porous separators in

---

Y. F. Zhou · S. Xie · C. H. Chen (✉)
Department of Materials Science and Engineering,
University of Science and Technology of China, Hefei,
Anhui 230026, China
e-mail: cchchen@ustc.edu.cn

Y. F. Zhou
School of Chemistry and Chemical Engineering,
Anhui University, Hefei, Anhui 230039, China

the hot gel electrolyte solution, and finally slowly cooling down to room temperature [3, 6–12]. This fabrication approach is complicated and all steps must be performed under the conditions of dry and oxygen-free atmosphere. In this paper, MMA monomer and the polymerization initiator are mixed with liquid electrolyte to form a liquid precursor and thus batteries can be first assembled by the relatively simple technology for conventional liquid electrolyte lithium batteries, followed by a thermal polymerization to obtain gel-polymer type lithium batteries. Successful realization of this new approach will provide a promising route for the industry of rechargeable lithium batteries.

Experimental

Preparation of gel-polymer lithium batteries

Methyl methacrylate (MMA) monomer (99.0%) was dehydrated by CaH_2 and then purified by underpressure distillation. The purified MMA and benzoyl peroxide (BPO) were mixed with commercial liquid electrolyte (LB302, 1 M solution of $LiPF_6$ in 1:1 EC/DEC) to form a precursor of GPE. The weight ratio of MMA: LB302 was from 1:4 to 1:1.25 while the amount of BPO was 0.5% of MMA. In order to identify the suitable gelation time, a portion of this liquid precursor was put in a sealed glass bottle that was then heated at 70 °C in an oven. It was observed that the liquid became immobilized after more than 2 h. Therefore, we used minimum 2–4 h as the polymerization time when making sample cells later. A porous polyethylene separator membrane was drenched with this precursor of GPE and CR2032 rechargeable button cells were prepared with metallic lithium anode, $LiNi_{0.8}Co_{0.2}O_2$ cathode (84 wt% $LiNi_{0.8}Co_{0.2}O_2$, 8 wt% acetylene black and 8 wt% polyvinylidene fluoride (PVDF), provided by Argonne National Laboratory) and the separator. Graphite anode with the composition of 91 wt% graphite and 9 wt% PVDF was also used to assemble full lithium-ion cells. Then these cells were heated at 70 °C for 2–4 h to form gel-polymer lithium batteries. For comparison, some $LiNi_{0.8}Co_{0.2}O_2$/graphite cells were also fabricated.

Electrochemical measurements

The conductivity and electrochemical stability window of GPEs were measured with a CHI604A electrochemical analyzer by the methods of AC impedance spectroscopy and cyclic voltammetry. The sample configuration for the AC impedance measurement was: SS(stainless steel)/GPE/SS, sealed in the form of CR2032 button cell. The applied frequency range was from 100 Hz to 100 kHz. The cell configuration for the cyclic voltammetry measurement was: SS/GPE/Li, the scan rate was 1 mV s^{-1}. The charge–discharge characteristics of $LiNi_{0.8}Co_{0.2}O_2$/GPE/Li, $LiNi_{0.8}Co_{0.2}O_2$/GPE/graphite and $LiNi_{0.8}Co_{0.2}O_2$/LB302/graphite button-cells (CR2032) were measured with a multi-channel cycler (Neware BTS-610).

Results and discussion

Ionic conductivity of polymerizing gel-polymer electrolyte

Figure 1 shows the ionic conductivity of the precursor mixture of GPE as the function of 70 °C-heating time.

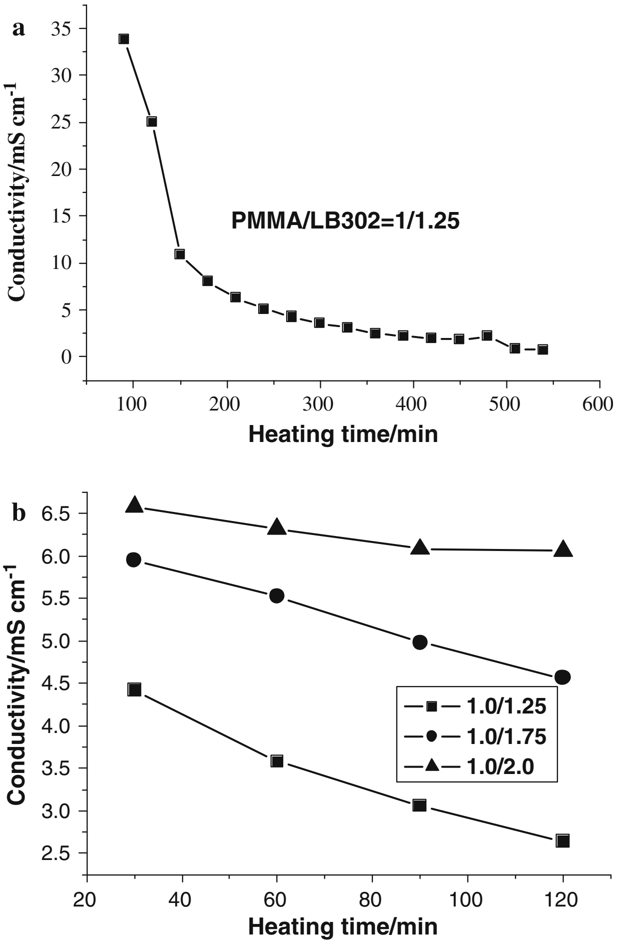

Fig. 1 Ionic conductivity changes with heating time from in-situ 70 °C measurement and the polymer to liquid electrolyte ratio PMMA/LB302 = 1/1.25 (**a**) and from intermittent measurements at 17 °C after every half-hour of 70 °C polymerization (**b**). The PMMA/LB302 ratio is indicated in the graph. Cell system: Stainless steel (SS)/GPE/SS

The conductivity was measured in two ways, i.e. in-situ measurement at 70 °C in order to continuously track the polymerization process (Fig. 1a) and intermittent measurement at 17 °C during the interval of every half-hour of polymerization at 70 °C (Fig. 1b). In both cases the conductivity decreases monotonously with increasing heating time. Obviously, an increase in the degree of polymerization of MMA must be accompanied with increasing viscosity of the gel and difficulty of ionic transportation in it. Furthermore, it is noticed from Fig. 1a that the majority of the conductivity drop at 70 °C takes place in the initial 2–3 h while only a small fraction of the total drop takes place in the rest of time. It can be concluded that the polymerization of MMA may have been nearly completed in the first several hours. Therefore, it is reasonable to take 2–4 h to prepare MMA based GPE at 70 °C. Besides, the ionic conductivity decreases with increasing PMMA/LB302 ratio. Nevertheless, in the PMMA/LB302 ratio range from 1.0/1.25 to 1.0/2.0, all of the PMMA-based GPEs show a conductivity of above 10^{-3} S cm^{-1}.

Figure 2 shows the conductivity changes of PMMA-based GPE with Li-salt content. PMMA/LB302 = 0 means there are no monomers in the electrolyte system. It can be seen that the conductivity of the GPE increases with the increase of Li-salt content in the precursor of GPE. When the amount of liquid electrolyte is more than 60 wt% (PMMA/LB302 ≤ 1.0/1.75 w/w), the conductivity increases slowly with the increase of Li-salt content in the GPE. On the other hand, the ability to immobilize liquid electrolyte is lowered with decreasing the PMMA/LB302 ratio. Hence, in order to compromise the mechanical strength and ionic conductivity of the GPE, the mass ratio of PMMA/LB302 ratio should be controlled in the range of 1/4–1/2.

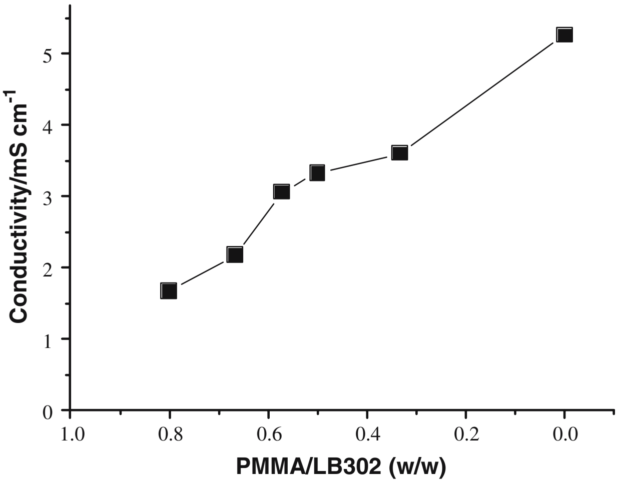

Fig. 2 Relationship between ionic conductivity of gel-polymer electrolyte and PMMA/LB302 weight ratio. All samples were heated at 70 °C for 2 h and then cooled to room temperature (17 °C)

Electrochemical stability window of PMMA based gel-polymer electrolyte

Figure 3 shows the cyclic voltammograms of two SS/electrolyte/Li cells, one with a typical PMMA based GPE (PMMA/LB302 = 1.0/2.0 w/w, Fig. 3a), another with liquid electrolyte (Fig. 3b) for comparison. The testing results of other samples with lower Li-salt content are similar to Fig. 3a and hence not given here. It can be seen that, in the voltage range between –0.4 and 4.0 V, compared with the cell using pure electrolyte (Fig. 3b), no extra cathodic or anodic peak is detected in the case of using PMMA based GPE (Fig. 3a). In fact, in the case of PMMA

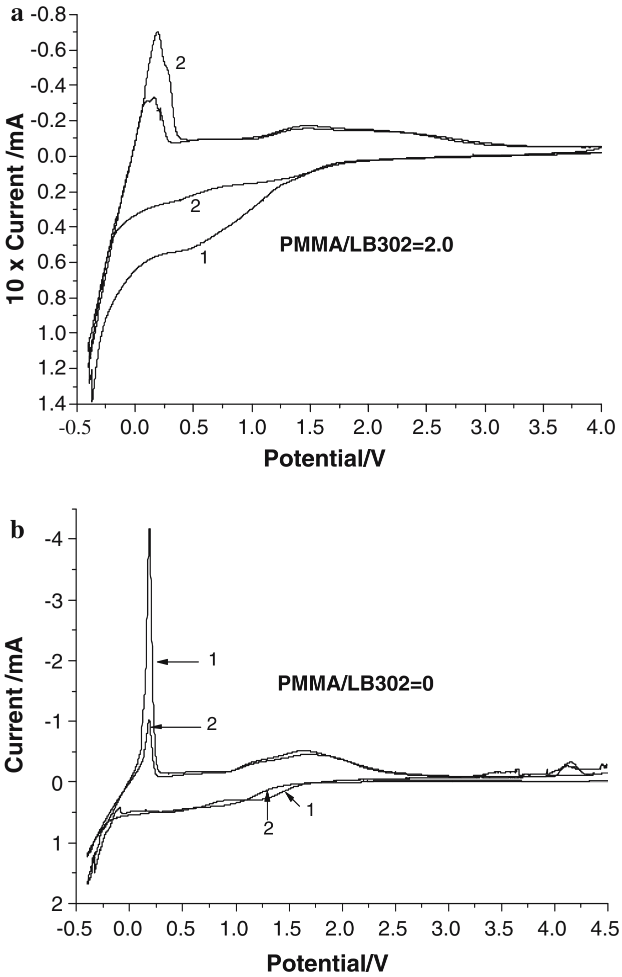

Fig. 3 Cyclic voltammograms of cells: SS/GPE/Li (**a**) and SS/LB302/Li (**b**) Scan rate: 1 mV s^{-1}

based GPE, measurement up to 4.2 V did not give rise to extra peaks either (not shown here). Therefore, the PMMA based GPE is stable from 0 up to 4.2 V (at least) vs. Li/Li^+. Besides, a significant cathodic peak and a significant anodic peak appear at the voltage around 0 V in both Figs. 3a and b. These two peaks can be obviously attributed to the plating and stripping of lithium on the stainless steel working electrode [14]. In addition, another couple of cathodic and anodic peaks is also observed around 1.5 V vs. Li/Li^+. Because a small amount of metal oxide (e.g. FeO) could be possibly formed on the SS surface out of natural oxidation, these two corresponding peaks can be attributed to the reduction and oxidation of the metal oxide on the surface [15, 16]. As is always the case for other metal oxide electrode, a substantial irreversibility for this process is also found in the first cycle.

The charge–discharge property of GPE based rechargeable lithium cells

Figures 4 and 5 show the charge–discharge property of a $LiNi_{0.8}Co_{0.2}O_2$/GPE/Li cell cycled at different current density. It is observed in either case (Figs. 4a, 5a) that at the beginning of first charging step the cell voltage reaches around 4.1 V rapidly and then drops sharply to about 3.9 V to start a usual charging process. Obviously, the initial cell impedance is large but becomes greatly reduced in a short time. As will be shown below (Fig. 6a), in contrast to these cells with lithium anode, this phenomenon of large initial cell impedance (LICI) is not observed in full cells with graphite anode. Therefore, the LICI must be related to the metallic lithium anode. Presumably an insulating layer could be formed on lithium surface. This layer might be detached and thus lead to the decrease of the

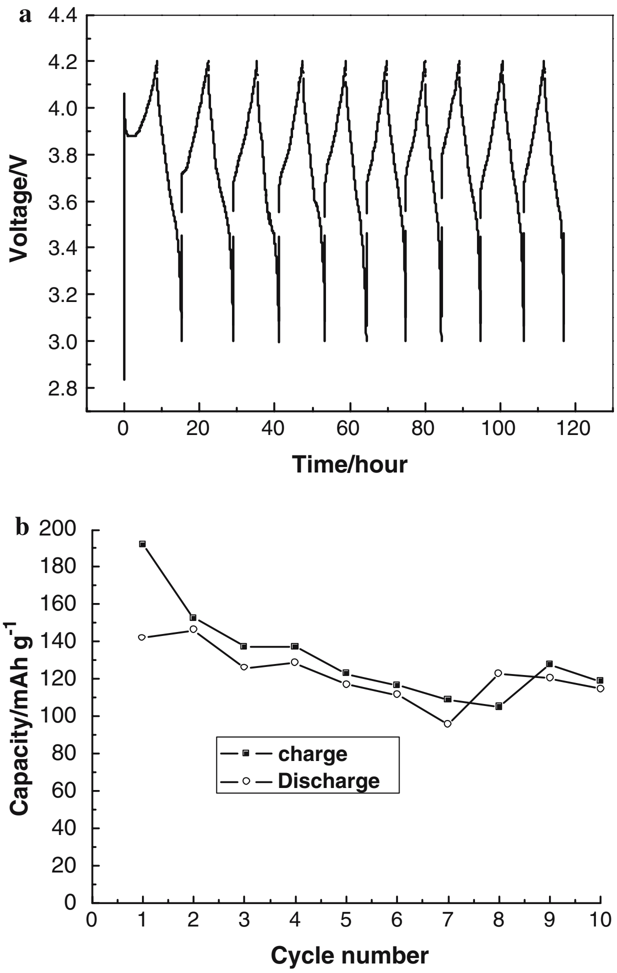

Fig. 4 Cycling performance of cell $LiNi_{0.8}Co_{0.2}O_2$/GPE/Li at 0.2 mA cm^{-2} current density. Cycling curves (**a**) and capacity-cycle number relationship (**b**). Here GPE was prepared with PMMA/LB302 = 1/4 and 70 °C polymerization for 2 h

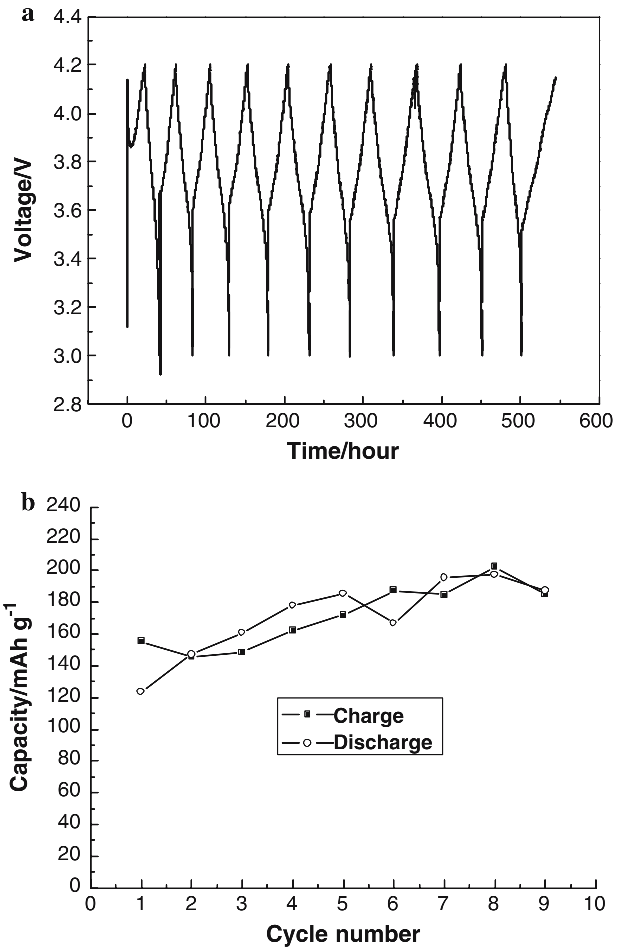

Fig. 5 Cycling performance of cell $LiNi_{0.8}Co_{0.2}O_2$/GPE/Li at 0.06 mA cm^{-2} current density. Cycling curves (**a**) and capacity-cycle number relationship (**b**). Here GPE was prepared with PMMA/LB302 = 1/4 and 70 °C polymerization for 3.5 h

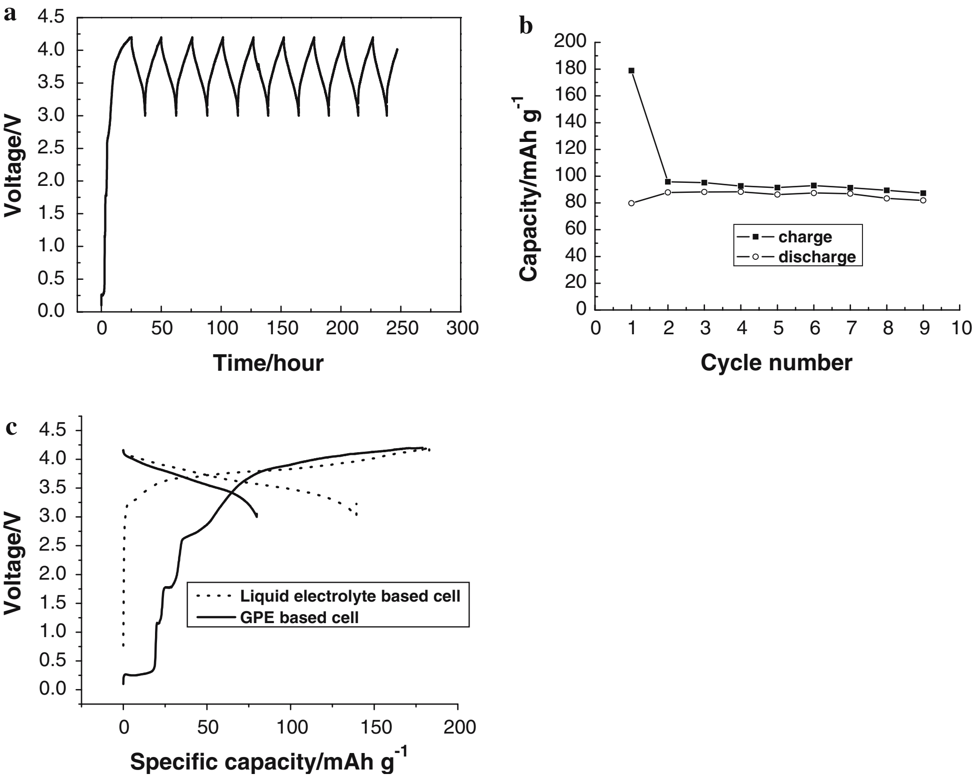

Fig. 6 Cycling performance of cell $LiNi_{0.8}Co_{0.2}O_2$/GPE/graphite at 0.06 mA cm^{-2} current density. Cycling curves (**a**) and capacity-cycle number relationship (**b**). Here GPE was prepared with PMMA/LB302 = 1/4 and 70 °C polymerization for 3.5 h. The cycling curve of first cycle is compared with that of a cell with LB302 liquid electrolyte (**c**)

cell impedance during the first charging process. Further investigation is needed to identify the presence of such a layer and its nature. Besides, depending on the current density, the cell capacity may either decrease (Fig. 4b) or increase (Fig. 5b) with cycle number in the subsequent charge–discharge cycles. Nevertheless, the trend of capacity decrease or increase is not maintained indefinitely; after some cycles, cells will reach normal capacity vs. cycle number characteristics similar to what would be observed in a $LiNi_{0.8}Co_{0.2}O_2$/LB302/Li cell.

Figure 6 shows the charge–discharge property of a $LiNi_{0.8}Co_{0.2}O_2$/GPE/graphite cell. It can be seen from Fig. 6a that the LICI phenomenon disappears here. Notice that the first charge capacity reaches 180 mAh g^{-1} with 4.2 V as the cut-off voltage (Fig. 6b). This specific capacity value (180 mAh g^{-1}) is almost the same as in the full cell with same cell chemistry yet using a liquid electrolyte (Fig. 6c). After a marked capacity loss (about 100 mAh g^{-1}) in the first cycle, the cycleability of the cell is rather good. The origin of this marked irreversible capacity loss may be hinted by comparing the first charge and discharge curves of the two cells with GPE and LB302 separately. In the cell with liquid electrolyte, almost all the reactions of lithiation and delithiation take place above 3 V of cell voltage. An irreversible capacity loss of about 35 mAh g^{-1} is observed. It is well established that this capacity loss can be attributed to the consumption of active lithium forming a SEI layer on graphite anode. On the other hand, in the cell with PMMA-based GPE, about four charge plateaus appear below 3 V of cell voltage in the first charge cycle. The overall capacity of these plateaus amount to about 65 mAh g^{-1}. Adding this low voltage capacity to the regular 35 mAh g^{-1} capacity loss, one should expect about 100 mAh g^{-1} capacity loss in the first cycle. This is exactly what is observed. The under 3 V plateaus could be related to the reactions between lithium and residual monomers, oligomers of MMA or even PMMA. For instance, the ester group ($-COOCH_3$) from MMA or PMMA might react with Li^+ from the cathode and electrons from graphite to form a ketol product [17]. More detailed reaction mechanism has been given in our study on gamma-ray irradiated GPE [18]. Figure 7 shows the AC impedance spectra of the $LiNi_{0.8}Co_{0.2}O_2$/graphite cells with liquid electrolyte and GPE after three formation cycles. The biggest difference of these two spectra is the medium-frequency semicircle. It has been established with a symmetric cell approach that the medium-frequency semicircle on the spectrum of $LiNi_{0.8}Co_{0.2}O_2$/LB302/graphite cell (Fig. 7a) is mainly contributed by the charge-transfer process between the cathode and the

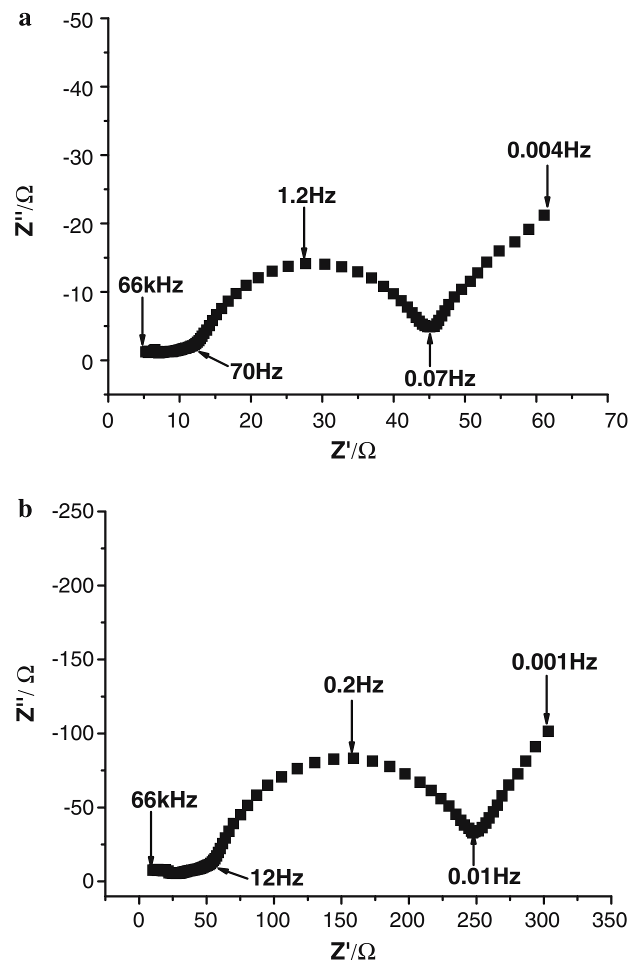

Fig. 7 AC impedance spectra of a cell $LiNi_{0.8}Co_{0.2}O_2$/LB302/graphite (**a**) and $LiNi_{0.8}Co_{0.2}O_2$/GPE/graphite (**b**) after three formation cycles. The frequency range was 0.001–100 kHz, electrode area: 1.54 cm^2 (OCV = 4.0 V)

electrolyte [19]. Therefore, in the case of PMMA-based electrolyte (Fig. 7b), the charge-transfer impedance between the cathode and the GPE is also much higher than that in the case of liquid electrolyte. The increase of the charge-transfer impedance can be attributed partly to the decrease of lithium ion conductivity of the electrolyte and partly to a possible more insulating surface layer formed on the $LiNi_{0.8}Co_{0.2}O_2$ cathode.

Conclusions

By heating the admixture of liquid electrolyte (LB302), MMA and BPO (initiator) at 70 °C, a PMMA-based GPE has been obtained. In the PMMA/LB302 ratio range from 1.0/1.25 to 1.0/2.0, ionic conductivity is above 10^{-3} S cm^{-1} at room temperature. Rechargeable lithium-ion batteries with PMMA based GPE can be fabricated through in-situ thermal polymerization. When metallic lithium is used as the anode, a LICI phenomenon is observed. This LICI phenomenon disappears in the case of using graphite anode. A significant irreversible capacity loss occurs in the first charge–discharge cycle. Most of capacity loss is related to multi-plateau processes under 3 V cell voltage. In addition, a large charge-transfer impedance between the cathode and the GPE has also been observed.

Acknowledgements This study was supported by the 100 Talents Program of Academia Sinica and National Science Fundation of China (50372064 and 20471057). We are also grateful to Dr. K. Amine from Argonne National Laboratory for providing $LiNi_{0.8}Co_{0.2}O_2$ and graphite laminates.

References

1. Meyer WH (1998) Adv Mater 10:439
2. Kim DW (1998) J Power Sources 76:175
3. Kim DW, Oh B, Park JH, Sun YK (2000) Solid State Ionics 138:41
4. Wang Y, Travas-Sejdic J, Steiner R (2002) Solid State Ionics 148:443
5. Song JY, Wang YY, Wan CC (1999) J Power Sources 77:183
6. Stephan AM, Thirunakaran R, Renganathan NG, Sundaram V, Pitchumani S, Muniyandi N, Gangadharan R, Ramamoorthy P (1999) J Power Sources 81–82:752
7. Kumar GG, Sampath S (2005) Solid State Ionics 176:773
8. Rhoo HJ (1997) Electrochim Acta 42:1571
9. Osaka T, Momma T, Ito H, Scrosati B (1997) J Power Sources 68:392
10. Tatsuma T, Taguchi M, Oyama N (2001) Electrochim Acta 46:1201
11. Choi NS, Park JK (2001) Electrochim Acta 46:1453
12. Kim CS, Oh SM (2002) J Power Sources 109:98
13. Jo SI, Sohn HJ, Kang DW, Kim DW (2003) J Power Sources 119–121:478
14. Xu W, Siow KS, Gao Z, Lee SW (1999) J Electrochem Soc 146:4410
15. Larcher D, Masquelier C, Bonnin D, Chabre Y, Masson V, Leriche JB, Tarascon JM (2003) J Electrochem Soc 150:A133
16. Shui JL, Zhang SL, Liu WL, Yu Y, Jiang GS, Xie S, Zhu CF, Chen CH (2004) Electrochem Commun 6:33
17. Barton D, Ollis D (1979) In: Sutherland IO (ed) Comprehensive organic chemistry, vol 2. Pergamon, Oxford, NY, p 934
18. Zhou YF, Xie S, Ge XW, Chen CH, Amine K (2004) J Appl Electrochem 34:1119
19. Chen CH, Liu J, Amine K (2001) Electrochem Commun 3:44